Catal Lett
DOI 10.1007/s10562-017-2097-2

Alkaline Earth (Ca, Mg) and Transition (La, Y) Metals Promotional Effects on Zn–Al Catalysts During Diethyl Carbonate Synthesis from Ethyl Carbamate and Ethanol

Kartikeya Shukla[1] · **Vimal Chandra Srivastava**[1]

Received: 10 March 2017 / Accepted: 29 May 2017

Abstract Diethyl carbonate, an important member in the family of organic carbonates, is a fuel additive like dimethyl carbonate (DMC). It holds an extra edge of having better gasoline/water distribution coefficient than DMC, and also DEC is widely used as an electrolyte in lithium ion batteries. Ethanolysis of ethyl carbamate (EC) is the most economical and greener route for DEC synthesis. Zn–Al–M (M=Ca, La, Mg and Y) have been synthesized using two methods and their activity have been explored DEC systhesis from EC and ethanol. The catalysts were characterized using thermogravimetric analysis, Brunauer, Emmett and Teller surface area, N_2 adsorption–desorption textural analysis, X-ray diffraction (XRD), Fourier transform infrared spectroscopy, temperature-programmed desorption (TPD), atomic-force microscopy and Raman spectroscopy. Pure metal oxides were observed during the XRD analysis and Al_2O_3 was found to be in amorphous form. Third metal oxide prepared from impregnation method was found to be present on the surface as well as in impregnated form. CO_2-TPD analysis showed close correlation between the basicity and the DEC yield. Zn–Al–Mg, prepared from precipitation method, being most basic, was found to be most effective although the performances of Zn–Al–Ca and Zn–Al–La were good. The effect of precipitants was also studied by synthesizing Zn–Al–Mg using NaOH and liquid NH_3 as precipitants. DEC yield of 40.2% and turn over frequency of 1055 $mg_{DEC}\ g_{cat}^{-1}\ h^{-1}$ was obtained in 5 h at 190 °C using Zn–Al–Mg prepared from precipitation method. Effect of reaction conditions was also studied and equilibrium constant of the reaction was estimated using the Benson group contribution method.

Electronic supplementary material The online version of this article (doi:10.1007/s10562-017-2097-2) contains supplementary material, which is available to authorized users.

✉ Kartikeya Shukla
kartikeyashr@gmail.com

✉ Vimal Chandra Srivastava
vimalcsr@yahoo.co.in; vimalfch@iitr.ac.in

[1] Department of Chemical Engineering, Indian Institute of Technology Roorkee, Roorkee, Uttarakhand 247667, India

Published online: 28 June 2017

Graphical Abstract

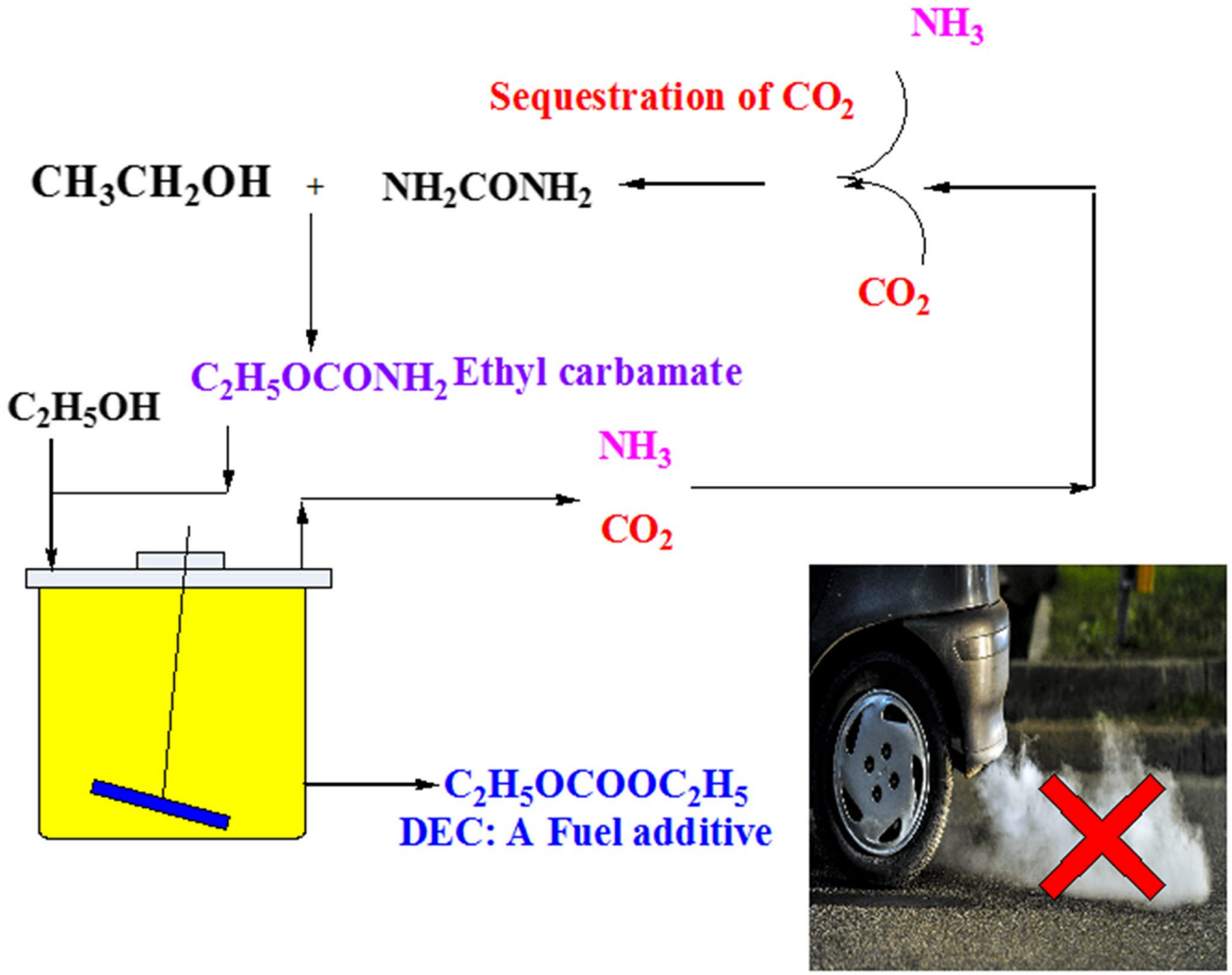

Keywords Diethyl carbonate · Ethyl carbamate · Synthesis methods · Catalysts · Precipitation · Characterization

1 Introduction

The sequestration of carbon dioxide (CO_2) into mineral carbonates has recently received much attention due to its indirect role as environment pollutant [1–3]. Many processes are being developed to transform CO_2 into valuable products such as syn gas by reforming of methane, synthesis of methanol from CO_2 and H_2, transformation of CO_2 to cyclic carbonates by cycloaddition with epoxides [4–7]. CO_2 is most oxidized state of carbon, the activation of CO_2 is the most difficult and stringent step in utilization of CO_2 [8]. Urea production is the most useful method for CO_2 fixation on a wide scale. Hence, utilization of urea to produce higher valued chemicals is another window of CO_2 utilization [9].

Organic carbonates are green class of compounds with a wide range of applications [10]. Dimethyl carbonate (DMC) and diethyl carbonate (DEC) are well known simple carbonates in the family [11]. They also hold important properties that of a fuel additive like commonly known methyl *t*-butyl ether (MTBE) and ethyl tert butyl ether (ETBE) [12, 13]. DEC, a colorless transparent liquid, besides being a fuel additive like DMC holds an extra edge of possessing better gasoline/water distribution coefficient. CH_3CH_2O– and –CO– groups present in DEC tend to make it more reactive helping in synthesis important chemicals [14]. Also DEC is widely used as a solvent in lithium ion batteries [15–17].

Phosgenation of ethanol is the oldest method which is discontinued owing to toxicity of phosgene. Various non-phosgene routes have been developed in the past decade. These include carbonylation of ethanol using CO_2

or urea, oxidative carbonylation of ethanol, transesterification of ethanol with organic carbonates, using ethyl nitrite route, etc. [12–26]. All the methods, various catalysts used and other engineering aspects have been critically reviewed earlier [27, 28]. Carbonylation of ethanol using CO_2 suffers from difficult activation of CO_2 which affects its thermodynamics. Trans-esterification of ethanol with DMC causes three azeotrope formation which hampers its recovery from the mixture. Urea ethanolysis, however, is an economical method due to its cheap raw materials and also because of no water formation during the process, and hence no azeotrope formation.

Ethanolysis of urea to synthesize DEC, is a two step process (shown by Eqs. 1 and 2), which deals with the formation of ethyl carbamate (EC) in first step followed by formation of DEC in second step (Eqs. 1 and 2).

$$C_2H_5OH + NH_2CONH_2 \rightarrow C_2H_5OCONH_2 + NH_3 \quad (1)$$

$$C_2H_5OH + C_2H_5OCONH_2 \rightarrow C_2H_5OCOOC_2H_5 + NH_3 \quad (2)$$

$$(C_2H_5O)_2CO + C_2H_5OCONH_2 \rightarrow C_2H_5OCONHC_2H_5 + C_2H_5OH + CO_2 \quad (3)$$

The process starts with urea which gives isocyanic acid, a very active compound, which reacts further with ethanol to give EC. The first step doesn't requires use of any catalyst while second step requires further use of catalyst. Formation of *N*-ethyl ethyl carbamate (NEEC) is also seen in trace as a byproduct (Eq. 3). Hence many studies have been reported on the synthesis of DEC from EC itself while only few investigators have focused on synthesis of DEC from urea. Various studies on the synthesis of DEC from EC have been summarized in Table S1 (supporting information) [29–38].

Previously reported studies on synthesis of DEC from EC include use of Zn and Pb based catalysts. However, no ternary oxides have been reported even for the synthesis of urea or EC. Hence, an attempt has been made in the present study to synthesize and characterize Zn–Al–M (M=Ca, La, Mg and Y) catalysts. The study is focused on understanding the effect of introducing third metal oxide into the fixed amount of Zn–Al hydroxides. The catalysts have been synthesized using precipitation and impregnation methods. Further, two different precipitants namely NaOH and liquid ammonia have been compared for their affect on the best performing catalysts. The catalysts have been characterized using various sophisticated instruments. These catalysts have been further used to synthesize DEC and study the effect on reaction conditions (temperature, time, catalysts wt% with respect to EC and ethanol/EC ratio) on DEC yield, EC conversion and turn over frequency (TOF).

2 Experimental

2.1 Materials

Magnesium nitrate hexahydrate, $Mg(NO_3)_2{\cdot}6H_2O$; cerium nitrate hexahydrate, $(Ce(NO_3)_3.6H_2O)$; and lanthanum (III) nitrate hexahydrate, $La(NO_3)_3.6H_2O$; yttrium nitrate hexahydrate, $Y(NO_3)_3.6H_2O$; and biphenyl of 99% purity was purchased from Sigma Aldrich; zinc nitrate hexahydrate, $(Zn(NO_3)_2.6H_2O)$ and aluminium nitrate nonahydrate $Al(NO_3)_3{\cdot}9H_2O$ of 99.5% purity was purchased from Hi media Laboratories, Mumbai. Sodium carbonate (Na_2CO_3) and sodium hydroxide (NaOH) was purchased from S.D Fine Chemicals Limited, and ethanol was purchased from Merck.

2.2 Preparation of Catalyst

Zinc nitrate hexahydrate and aluminium nitrate nonahydrate were dissolved in Millipore water and mixed drop wise in the molar ratio of 3:1. 3 M NaOH solution was mixed drop wise to the mixed solution under vigorous mixing at 10 pH. The formed precipitate was aged at 80 °C at 4 h and further for 24 h at room temperature. The precipitate was filtered and washed several times with deionised water till the pH of filtrate reached till 7. The precipitate was dried at 80 °C for 24 h. The formed Zn–Al hydroxide was prepared for calcined to get binary oxides.

2.2.1 Method A

Twelve gram of prepared hydroxide was dispersed in deionised water. Similarly, other metal nitrates which include magnesium, yttrium, calcium and lanthanum nitrate were dispersed in deionised water such that the metal weight was 1 g. Both the solutions were mixed drop wise and the pH was adjusted to ten with the help of drop wise addition of 3 M NaOH solution. The precipitate was washed with deionised water till the pH of the filtrate became 7. The precipitate was aged at 80 °C and dried at 110 °C for 24 h followed by calcination to remove other type of impurities and convert all types of hydroxyl groups to oxides. The catalysts prepared by method A are represented by Zn–Al–M–A (M=Ca, Mg, La and Y).

2.2.2 Method B

Prepared hydroxide already was calcined at 700 °C to get the final form of oxides. 1 g of prepared Zn–Al oxides were

impregnated with the third nitrate solutions and the solution was stirred vigorously for 24 h. The third nitrate solution was taken in such a way that the metal weighed ≈0.5 g. The solutions were dried at 110 °C for 24 h and were further calcined at 700 °C. The catalyst prepared by method B were represented by Zn–Al–M–B (M=Ca, Mg, La and Y).

Further Zn–Al–Mg–C catalyst was also prepared by first method but using liquid ammonia as precipitant. Firstly Zn–Al hydroxides were prepared and then the third element was precipitated using liquid ammonia as precipitant.

2.3 Catalyst Characterization

Thermogravimetric analysis (TGA) of the synthesized catalysts was carried out with SII 6300 EXSTAR analyzer. The temperature range was set in the range of 30–1000 °C with a heating rate of 10 K/min.

The prepared catalysts were characterized by X-ray diffraction (XRD) (Bruker D8 ADVANCE) using Cu-K_α radiation (l = 0154 nm). This was done with X-ray gun operated at 40 kV and 30 mA. The 2θ values were varied in the range of 5–90° with step size of 0.02°. PANalytical Xpert high score software along with the Joint committee on powder diffraction international centre for diffraction data (JCPDS-ICDD) library was used for identification of crystalline phases. Scherrer equation was used for the calculation of average crystalline size.

To observe the textural properties such as surface area and pore volume, liquid nitrogen (−195 °C) adsorption–desorption method was used. Data were generated using Micromeritics ASAP 2020 instrument. Brunauer–Emmett–Teller (BET) model was used for surface area analysis.

Basicity measurements of the catalysts were obtained by carrying out (CO_2) temperature programmed desorption (TPD) analysis using Micromeritics ChemiSorb 2720 instrument, USA. The catalysts were placed in quartz U-tube reactor and degassed at 200 °C under N_2 flow (20 cm^3 min^{-1}) for 2 h. For CO_2-TPD, Micromeritics Chemisorb 2720 instrument with thermal conductivity detector (TCD) was used. The catalysts were placed in quartz U-tube and pretreated at 200 °C under N_2 flow (20 cm^3 min^{-1}) for 2 h. CO_2 adsorption for 1 h was followed by desorption, whose profiles were recorded in the range of 50–800 °C with a heating rate of 10 °C/min under helium flow (20 cm^3 min^{-1}) and the evolved CO_2 was monitored with a TCD.

Zn–Al–Mg–A and Zn–Al–Mg–C synthesized from first method were also characterized by Raman spectroscopy equipped with Olympus BX series optical microscope. The catalysts were scanned within the range 0–1300 cm^{-1} of Raman line frequency.

Fourier transform infrared (FTIR) spectroscopy was used to find out the surface functional groups of the fresh, regenerated catalysts, catalyst interacted with EC, and the reaction solution by using a FTIR spectrophotometer (Thermo Nicolet, Model Magna 760). Catalyst interacted with EC was prepared by blending EC (1.8 g) with the catalyst (0.18 g) and heating the pellet for 3 h at specified temperature (100–140 °C). The solid catalyst was recovered by centrifuging the reaction solution. The catalyst was further washed with de-ionised water and ethanol three times followed by drying at 110 °C overnight. Thereafter the catalyst was further activated by calcination 700 °C.

The structural morphology of fresh and regenerated catalyst was also studied using atomic-force microscopy (AFM) of M/s molecular tools and devices for nanotechnology (NT-MDT) coupled with NOVA software for image analysis. The samples were prepared in ethanol in which 20 mg of sample dispersed in 10 mL ethanol solution, which was sonicated for 120 min followed by small dispersion of solution on a glass plate. The plate was dried, at room temperature, overnight. This glass plate was then, used for AFM analysis.

2.4 DEC Synthesis from Ethanol and EC

DEC synthesis reaction was carried out in 50 mL high pressure autoclave. 1.8 g of EC (0.02 moles), 12 mL ethanol and the catalyst (0.18 g) were charged into the autoclave. The autoclave was purged with nitrogen so as to remove any air present in the reactor. The reactor was pressurized up to 4 Mpa and heated to the required temperature. The ammonia was removed at regular interval which was produced during the synthesis. The reactor was cooled to room temperature after the completion of the reaction followed by separation of catalyst using centrifuge. The liquid mixture was analyzed using gas chromatograph (NETEL Michro-9100) equipped with Optima Wax capillary column having length 30 m and internal diameter 0.25 mm. DEC yields of products was calculated using the following formula:

$$Y = \frac{\text{Moles of product formed}}{\text{Moles of EC taken}} \times 100\% \quad (4)$$

where, Y is the yield of DEC or NEEC.

3 Results and Discussion

3.1 Characterization of Catalyst

3.1.1 TG-DTA

To analyze the nature of precursor of the catalysts, TG-DTA study was conducted whose plot is given in Fig. S1 (Supporting Information). TG profile seems to be quite similar to that reported in the literature for ZnO and Al_2O_3 [39, 40]. Weight loss below 250 °C may be due to loss of OH^- ions and dehydration of surface adsorbed water [41]. As the catalysts were thoroughly washed by double distilled water, therefore, many ions were removed and hence, no drastic loss in weight was observed as are usually observed when the catalyst are prepared from sol–gel method. Usually the weight loss must be accompanied by endothermic peak, but the smoothness of TGA curve may be due to crystallization of ZnO which is exothermic in nature. No significantly weight lost was observed beyond 650 °C. Hence it was selected as the optimum calcination temperature in order to convert the precursors into their final forms.

3.1.2 XRD

The XRD pattern of the catalysts prepared by method A and B are shown in Fig. 1a, b. Al_2O_3 was found to occur in amorphous form. The patterns were matched with ICDD library and presence of pure phase was found to exist in all the catalyst. Since Al_2O_3 can be seen in EDX analysis in Table 1, hence, it can be inferred that it was present in amorphous form. Pure phases of ZnO, CaO, Y_2O_3 and La_2O_3 were identified to be present in crystalline form in the catalysts (shown in Fig. 1) with the PDF-ICDD of 01-076-0704, 00-023-1009, 00-048-1467, 01-083-0927 and 01-083-1348, respectively. Most intensive peak was identified and used for the calculation of crystallite size. Crystal size of the catalysts decreased with the insertion of third element in the Zn–Al oxide catalyst. CaO, MgO and Y_2O_3 were found to be in crystalline form in the catalysts prepared by first method. Zn–Al–La was found to be mostly in amorphous state as compared to others. Zn–Al–La prepared from impregnation method was observed to contain both Al_2O_3 and La_2O_3 in amorphous and impregnated form.

3.1.3 Textural Properties

Table 1 summarizes the BET surface areas of the synthesized catalysts. Ternary oxides synthesized by first method were found to possess more surface area than that possessed by catalysts prepared from second method. The plugging of pores of Zn–Al oxide with the third element was also responsible for decrease in BET surface area in the catalysts prepared by impregnation method.

Adsorption/desorption isotherm is shown in Fig. 2a. The catalysts synthesized can be termed as mesoporous materials and classified to follow type IV and V [42]. This confirms the presence of mesopores and absence of micropores in the synthesized catalysts. The pores of Zn–Al–Mg oxides synthesized using ammonia precipitant and NaOH precipitant were found to possess H3 and H4 hysteresis have slit-shaped pores with the latter having narrower one. It can be seen that capillary condensation occurs within micropores when relative pressure increases ($P/P_o > 0.65$).

3.1.4 CO_2-TPD Analysis

CO_2-TPD curves of the catalysts are shown in Fig. 3a, b. The catalysts were further categorized by their base strength and basicities. Base strength is represented by the desorption temperature while the quantity of CO_2 desorbed signifies the basicity of the catalyst [43]. Catalysts base strength was categorized as weak sites (<200 °C), moderate sites (200 °C < T < 550 °C) and strong sites (>550 °C). Weak sites are due to presence of OH^- groups, medium sites are due to Mn^+–O^{-2} while strong sites are due to presence of O_2^{2-} [44, 45]. All the catalysts were found to possess strong basic sites, and high base strength, since the quantity of Zn and Al was found to be greater than the third metal oxide. Ternary oxides prepared by precipitation method were found to be more basic as compared to the catalysts prepared by impregnation method. This may be due to blocking of some pores by third metal oxide during impregnated into the catalyst which can also be observed by witnessing shoulder peaks in CO_2-TPD profile of case of Zn–Al–M–B catalysts. Zn–Al–Mg was found to have maximum basicity among all ternary oxides in the range stated above.

3.1.5 Raman Spectroscopy

Raman spectra of ternary oxides of Zn–Al–Mg–A and Zn–Al–Mg–C prepared using two different precipitating agents (NaOH and NH_3) is shown in Fig. 4. The spectrum Zn–Al–Mg–A revealed two high intensity peaks at 99 and 437 cm^{-1} corresponding to the E2L and E2H modes of hexagonal ZnO, respectively. The Raman peak observed at 1065 cm^{-1} is attributed to the A1(TO) + E1(TO) + E2L multi photon scattering mode. In addition, as-prepared ternary oxide also displayed few weak intensity peaks at 150, 330, 480, and 607 cm^{-1} which can be assigned to 2E2L, 3E2H–E2L, E1(TO) + E2L and 2(E2H–E2L) mode, respectively [46]. The presence of oxide of aluminum is evident from a low intensity shoulder peak at 375 cm^{-1} [47]. The Raman spectrum of Zn–Al–Mg–C is similar to that of

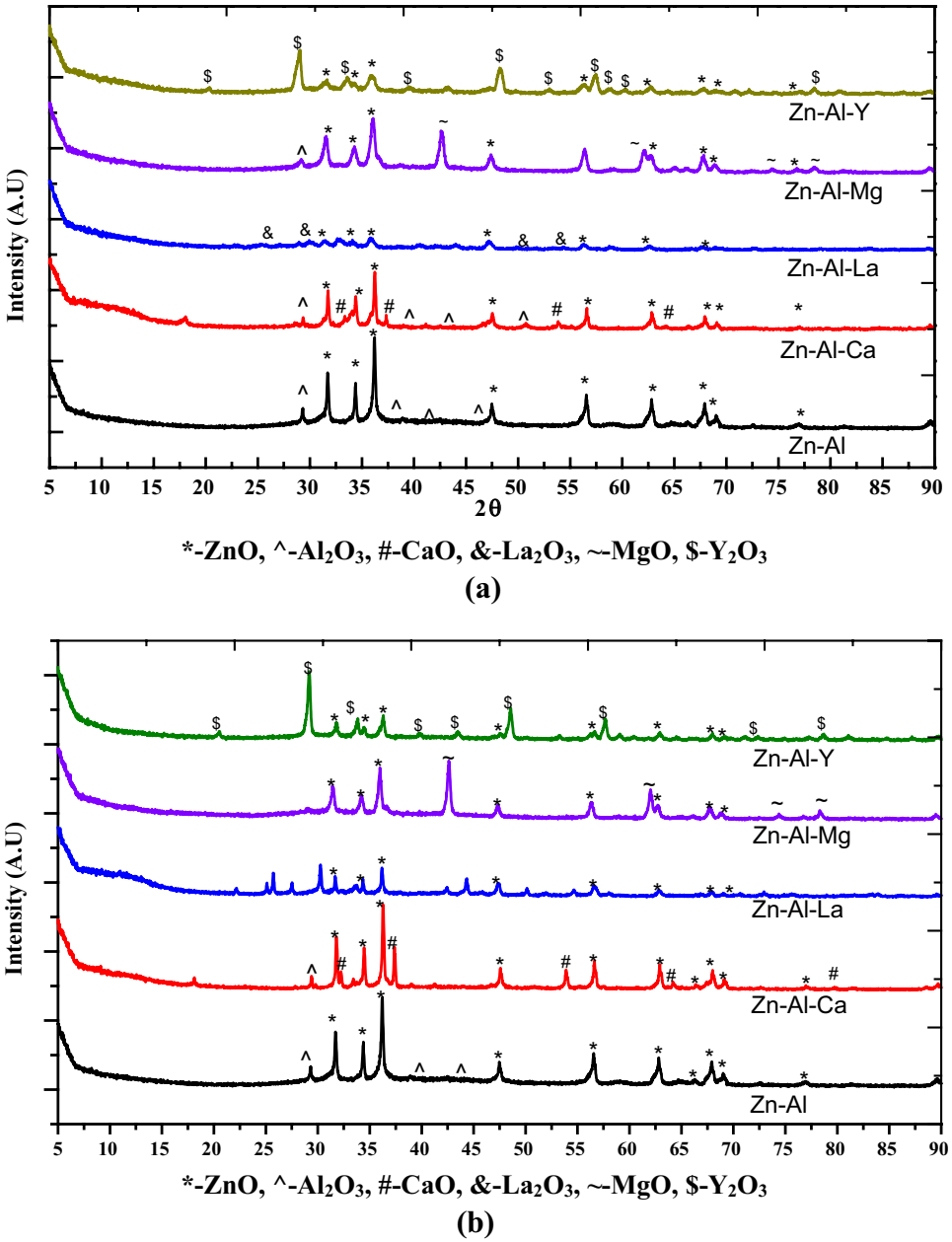

Fig. 1 XRD patterns of catalysts prepared by **a** precipitation (Zn–Al–M–A), and **b** impregnation (Zn–Al–M–B) methods

Zn–Al–Mg–A except that the peak observed for multi photon scattering mode is observed at 1080 cm^{-1} instead of 1065 cm^{-1} which can be due to the difference in the nature of precipitating agent.

3.1.6 FTIR Analysis

FTIR spectra of fresh, recovered and EC interacted catalysts are shown in the Fig. 5a. Peaks at 3461, 1642, 1386 and 1115 cm^{-1} as present in the fresh catalyst are also seen in the regenerated catalysts. The regenerated catalyst also shows peaks around 2320 and 1580 cm^{-1} which are due to isocyanate, N=C=O stretch and N–H bend of amide. Peak around 2320 cm^{-1} signifies the formation of $Zn(NCO)_2$ which is not witnessed in the regenerated catalyst. This might have formed from the reactions 5 and 6 as suggested by An et al. [31].

$$NH_2OCOC_2H_5 \rightarrow HNCO + C_2H_5OH \quad (5)$$

$$ZnO + HNCO \rightarrow Zn(NCO)_2 + H_2O \quad (6)$$

The same peak is also witnessed in the reaction solution emphasizing the formation of isocyanate during the reaction (Fig. 5b). The peak at ≈1273 cm^{-1} is due to the C–O–C stretch of dialkyl group in the reaction solution. The peak at ≈1033 cm^{-1} shows the C–O stretch of ethanol.

Table 1 DEC yield and selectivity using various synthesized catalysts

Catalyst	B.E.T surface area (m^2/g)	DEC yield (%)	NEEC yield (%)	EC conversion (%)	TOF ($mg_{DEC}\ g_{cat}^{-1}\ h^{-1}$)	Crystallite size (nm)	Elemental analysis (EDX)			
							Zn	Al	M	O
Zn–Al	36	20.1	0.2	26.4	526.6	47.7	48.11	11.67	–	40.22
Zn–Al–Ca–A	28	32.5	0.4	42.6	852.2	39.5	14.99	1.11	28.77	55.13
Zn–Al–La–A	30	23.2	0.4	28.2	507.4	18.1	40.51	3.5	28.17	27.82
Zn–Al–Mg–A	31	40.2	0.6	50.8	1055.2	19.1	58.41	4.19	0.55	36.85
Zn–Al–Y–A	28	30.2	0.2	38.1	792.2	16	39.88	5.75	7.18	47.19
Zn–Al–Ca–B	15	21.2	0.1	28.8	555.5	38.7	33.68	10.11	10.47	45.74
Zn–Al–La–B	18	19.4	0.2	24.5	508.8	44	60.94	9.35	11.17	18.54
Zn–Al–Mg–B	21	28.2	0.1	36.7	747.7	28	69.77	4.76	–	25.47
Zn–Al–Y–B	18	25.2	0.2	31.8	661.1	29	54.36	8.64	7.18	29.82
Zn–Al–Mg–C	28	35.6	0.4	48.8	934.4	–	–	–	–	–

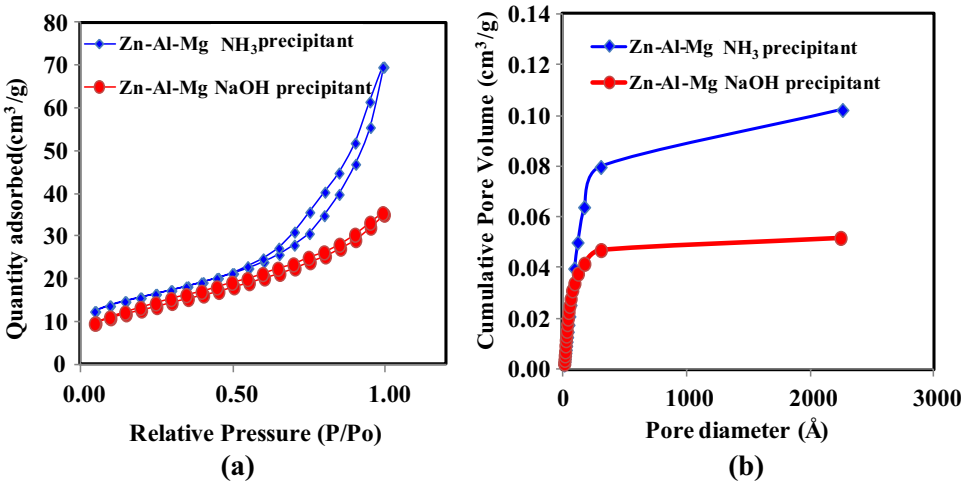

Fig. 2 **a** Liquid nitrogen adsorption–desorption isotherm, and **b** pore size distribution of the Zn–Al–Mg catalysts

3.1.7 Surface Morphology and Elemental Analysis

The surface morphologies and elemental analysis were studied using AFM technique. Surface elemental compositions of various catalysts are shown in Table 1. Zn–Al–Mg–A was the best performing catalyst among all the prepared catalysts. Hence, it was chosen to study the surface morphology by AFM technique, the size of fresh and regenerated Zn–Mg–Al–A catalyst after the third reaction. The distribution of catalysts sizes were studied over whole surface of the catalysts. It can be seen from Fig. 6a, b, that the catalysts size was not as evenly distributed in the recovered catalyst as it was in fresh catalyst. Catalyst agglomeration was also slightly observed after recovery of the catalyst for the third time (as seen in Fig. 6c).

3.2 Catalytic Activity

Basic strength and basicity have profound effect on DEC yield and hence have been examined carefully. Basic strength, a measure of temperature up to which a site can retain CO_2 molecule, and basicity, a measure of the basic sites present on the catalyst, can be seen from Fig. 3 and Table 2. All the catalysts possessed mild and strong basic sites. The sites are mostly strong as they desorbed CO_2 at temperature greater than 400 °C. Table 1 summarizes the results of the screening study of the catalysts. DEC yields obtained were seemed to be dependent on the basicity of the catalysts. Zn–Al–M–A catalysts were found to give better yield than the Zn–Al–M–B type catalysts. This may be due to higher basicities of 'A' series of catalysts as compared to 'B' type catalysts. Plugging of pores was found to occur in 'B' type catalysts. CO_2-TPD clearly shows shoulder peak which is attributed to the impregnation of third metal oxide within the pores of the catalysts.

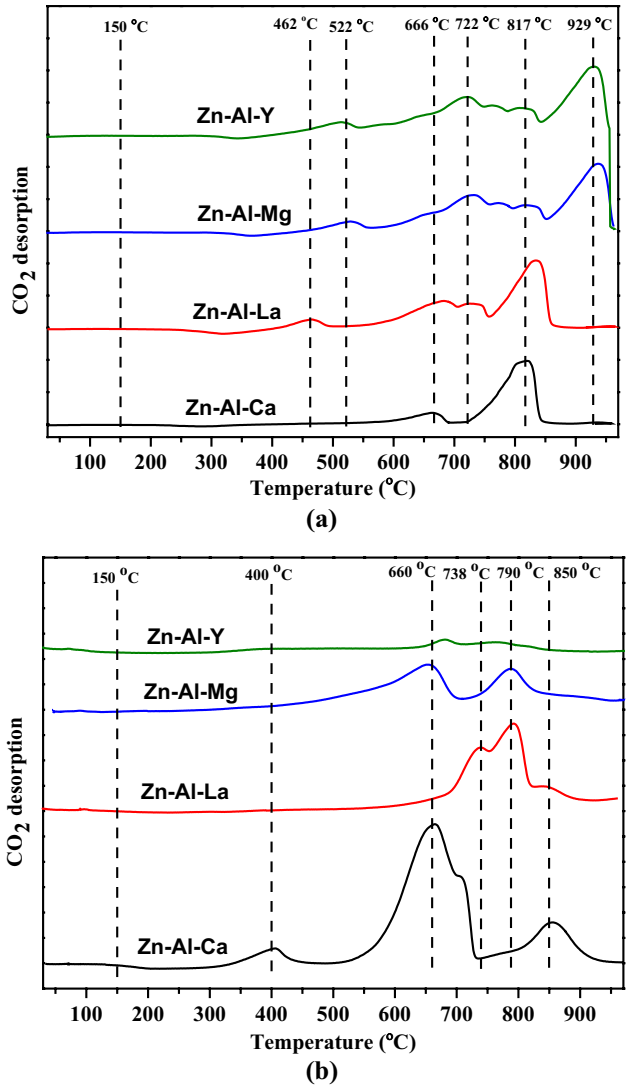

Fig. 3 CO_2-TPD profiles of Zn–Al–M catalysts prepared by **a** precipitation and **b** impregnation method

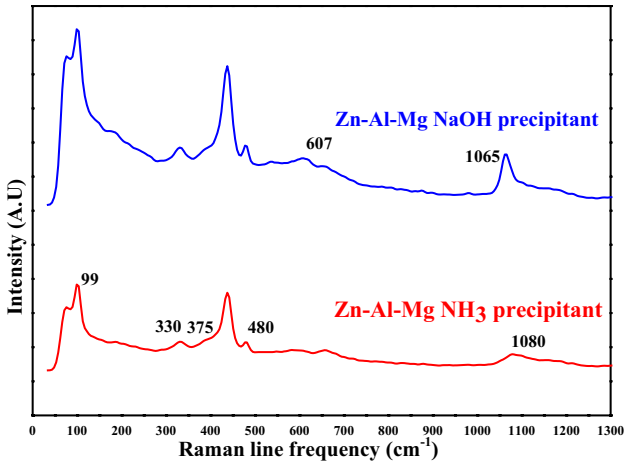

Fig. 4 Raman spectra of Zn–Al–Mg catalysts synthesized by A method using NaOH and liquid ammonia as precipitants

Yield obtained with Zn–Al–Mg–C was close to Zn–Al–Mg–A. It means the effect of precipitant doesn't affects the yield and DEC selectivity substantially. This can also be seen from Fig. 4, which shows almost same Raman profile suggesting almost equal defects created in the catalysts. The decomposition of EC as suggested by Eqs. 5 and 6, which was also witnessed in the FTIR spectra, leads to the formation of HNCO and ethanol. This contributes to the loss in mass of raw material as undesired products (Table 1). Zn–Al–Mg–A was found to be the best after screening among various catalysts. Hence it was chosen to study the effect of different operating conditions.

The general mechanism of the reaction, proposed for Zn–Al–Mg–A, is shown in Fig. S2 (supporting information). It can be seen from Fig. 1a, all the three oxides (Zn, Al and Mg) were found to co-exist in the synthesized catalyst. ZnO and MgO were found mostly in crystalline form as compared to Al_2O_3. Activation of ethanol occurs at the oxygen site of the oxides. Carbonyl group of ethyl carbamate is adsorbed at the metal sites of the catalysts. The ethoxy group attacks the electrophilic site of carbon to replace NH_2 group with it thereby producing DEC and NH_3.

3.2.1 *Effect of Operating Parameters*

The effect of temperature (453–483 K) on DEC yield and EC conversion was studied (Fig. 7a). The conversion of EC and yield of DEC increased up to 463 K and remained the same at 483 K. Theoretically equilibrium constants of DEC synthesis from EC, varying with temperature, was also studied. Standard molar entropy change of DEC and EC was estimated using the Benson group contribution method [48]. The coefficients of heat capacity of the reaction and products components were estimated using Ruzicka and Zabranski model [49]. Equilibrium constant was found to be increase abruptly after 150 °C as shown in the Fig. S3a. Hence it is advisable to conduct reaction beyond this temperature. EC conversion was found to be increase with an increase in temperature but DEC yield was almost the same for 190 and 200 °C as shown in the Fig. 7a. This may be due to the increase in rates of side reaction leading to the formation of N-EEC.

The effect of time on the DEC yield was studied in the range of 1–6 h and the results are shown in the Fig. 7b. The yield of DEC and EC conversion increased up to 5 h and thereafter they were constant. This may be attributed to the reaction approaching equilibrium. Increasing the time will deprive TOF of the reaction and hence 5 h was chosen to be the optimum time for DEC synthesis.

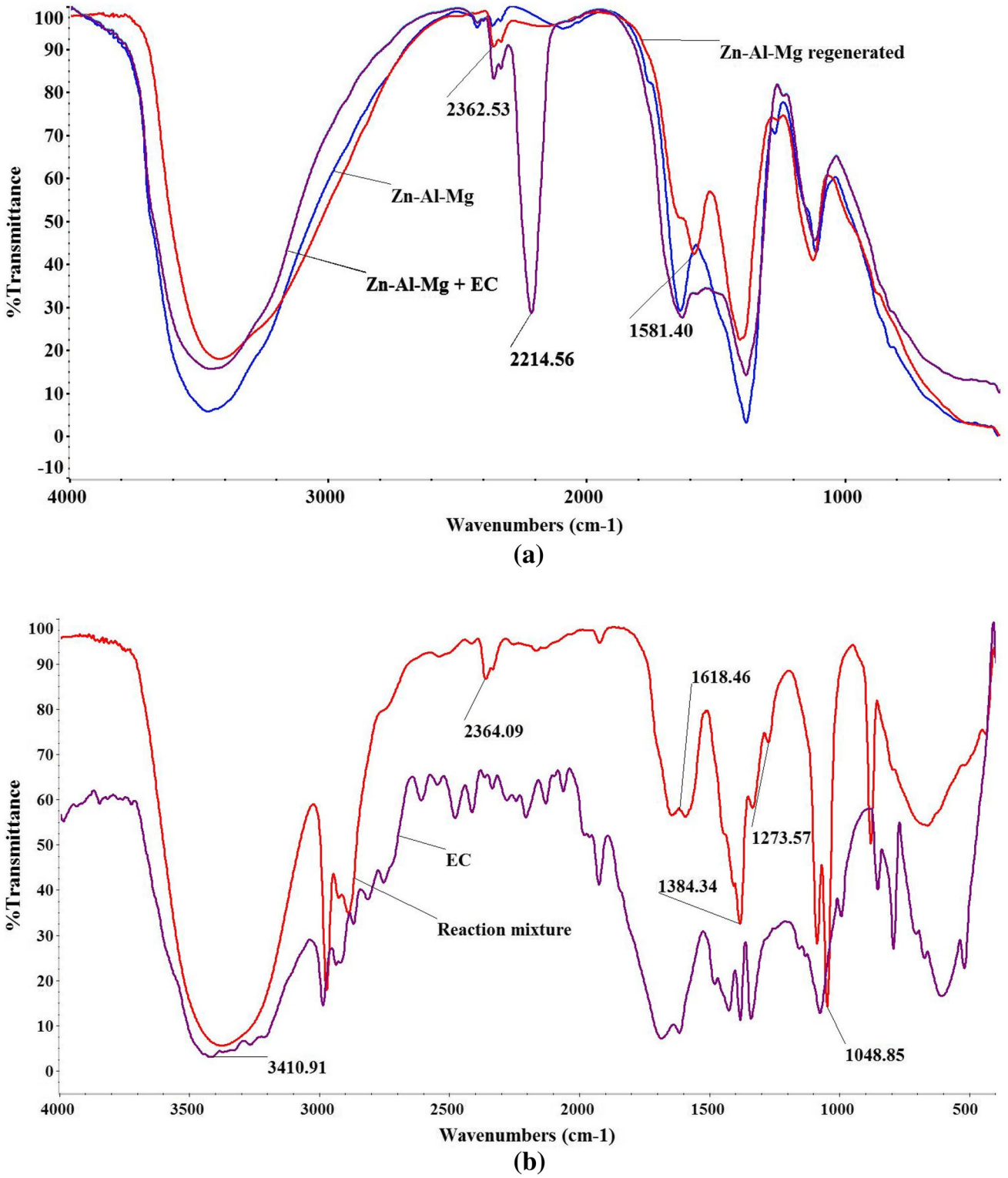

Fig. 5 FTIR spectra of **a** Zn–Al–Mg fresh, regenerated and interacted catalyst, **b** EC and reaction solution

The effect of catalyst wt (by weight% of EC) was studied in the range of 5–15. Figure 7c shows that the conversion of EC increased abruptly when catalyst concentration was increased from 5 to 10 wt%. On further increasing the catalyst concentration, change in conversion of EC and yield of DEC was very low. This may be attributed to the reaction

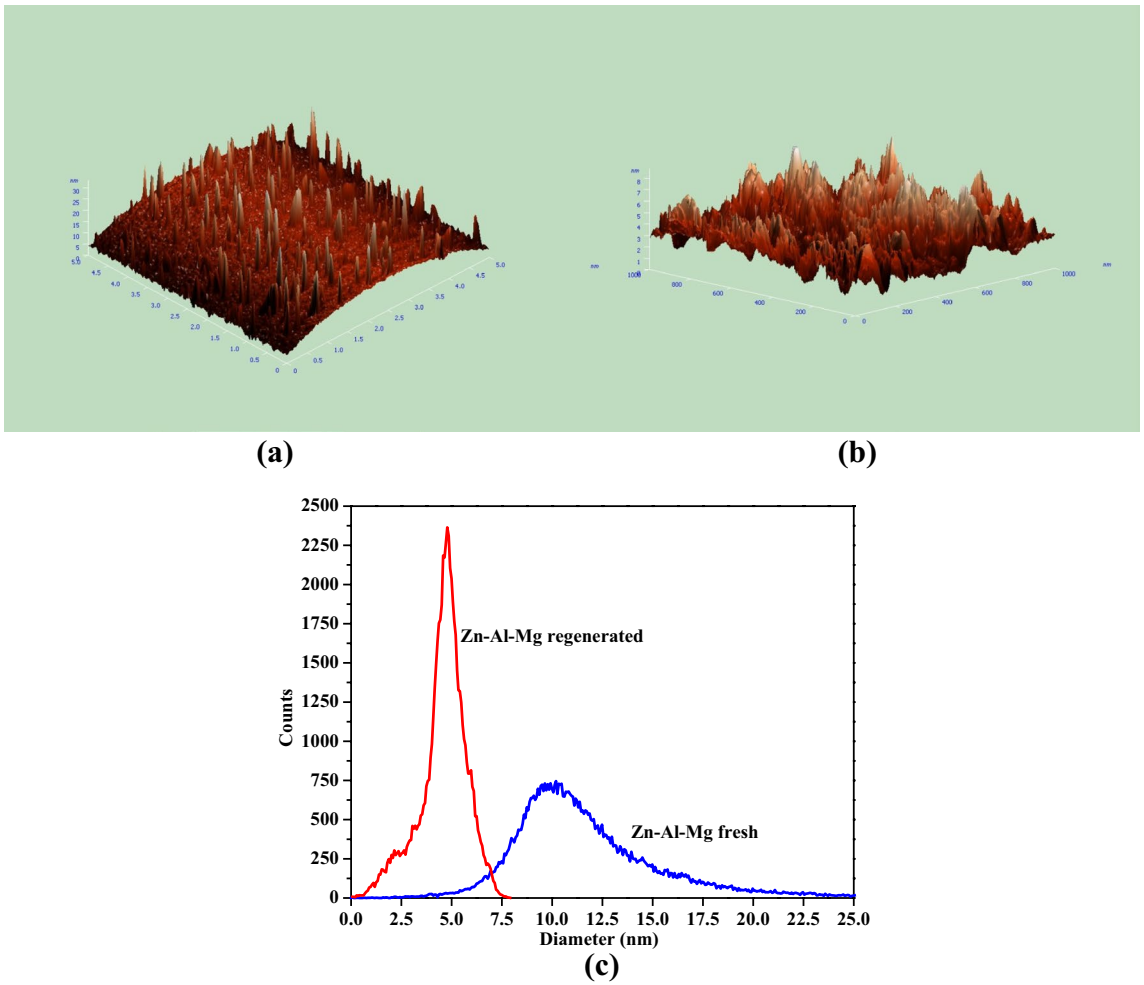

Fig. 6 **a** AFM—image of Zn–Al–Mg precipitation fresh catalyst, **b** AFM—image of Zn–Al–Mg precipitation regenerated catalyst and **c** catalysts size of fresh and regenerated Zn–Al–Mg precipitation catalyst

Table 2 CO_2-TPD classification of various catalysts

Catalysts	Basicity or amount desorbed CO_2 (mmol g^{-1})			
	Weak sites (<200) °C	Medium sites (200–550) °C	Strong sites (>550) °C	Total basicity
Zn–Al–Ca–A	0.04 (150 °C)	0.02 (462 and 522 °C)	0.15 (666 and 817 °C)	0.21
Zn–Al–La–A	0.04 (150 °C)	0.06 (462 °C)	0.13 (666, 722, 929 °C)	0.2
Zn–Al–Mg–A	0.04 (150 °C)	0.06 (522 °C)	0.15 (666, 722, 817 and 929 °C)	0.25
Zn–Al–Y–A	0.04 (150 °C)	0.06 (522 °C)	0.14 (666, 722, 817 and 929 °C)	0.24
ZnAl–Ca–B	0.04 (150 °C)	0.06 (400 °C)	0.13 (660 and 850 °C)	0.23
Zn–Al–La–B	0.04 (150 °C)	0.02 (400 °C)	0.11 (738 and 790 °C)	0.17
Zn–Al–Mg–B	0.03 (150 °C)	0.02 (400 °C)	0.13 (660 and 790 °C)	0.18
Zn–Al–Y–B	0.04 (150 °C)	0.02 (400 °C)	0.05 (660 and 790 °C)	0.11

approaching thermodynamic or equilibrium conversion. Hence, 10 wt% was chosen to be the optimum catalyst concentration for DEC synthesis from EC.

The effect of ethanol/EC ratio was studied in the range of 5–20 (Fig. 7d). Clearly, ethanol/EC ratio of 10 was found to be better than others when DEC yield was considered. This optimum ethanol/EC ratio was found to be similar to that reported in the literature [16]. Lower ethanol/EC ratio increases EC concentration and hence it increases the *N*-ethylation of EC. By raising the ethanol/ EC above

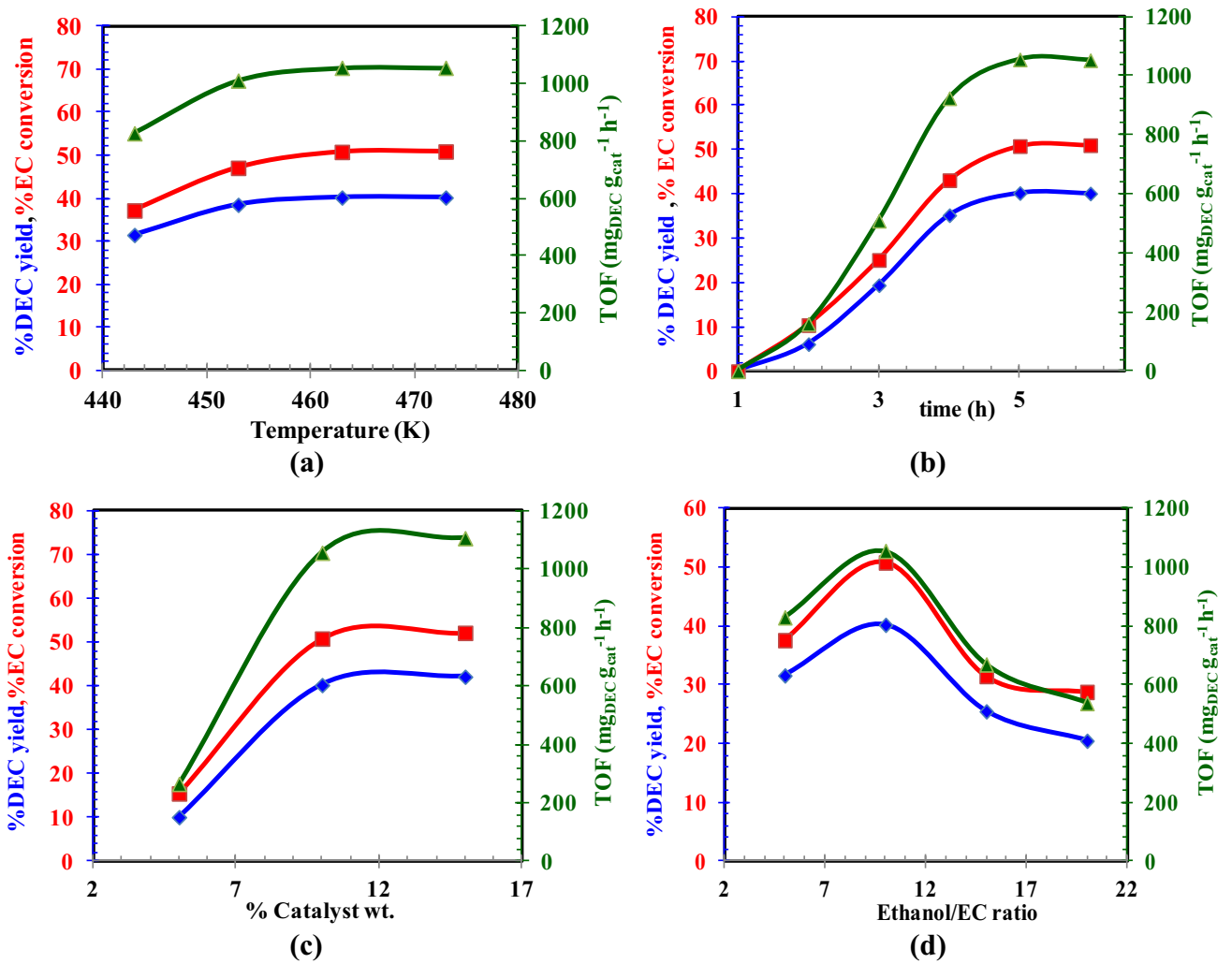

Fig. 7 Effect on operating parameters on DEC yield (*blue diamond*), EC conversion (*red square*) and TOF (*green triangle*) using Zn–Al–Mg–A catalyst. **a** Temperature (443–473 K), **b** time (1–6 h), **c** catalyst weight (5–15 wt%), and **d** ethanol/EC ratio (5–20)

optimum value, the reaction will be pushed to the product side by Le Chatelier principle. At too higher ethanol/EC ratio, the catalytic sites get covered with ethanol and hence can't be accessed by EC.

3.2.2 Catalysts Regeneration and its Reusability

Zn–Al–Mg–A was the best catalyst for the synthesis of DEC from EC owing to its high basicity and high surface area. The catalyst was successfully regenerated, even after third time, which can be shown in Fig. S3b. Almost same peaks, as that of fresh Zn–Al–Mg–A, were obtained in XRD and FTIR. Hence its activity was studied after regeneration. The catalyst was observed to be reusable for three times with TOF of 1055.2, 1050 and 998 $mg_{DEC}\ g_{cat}^{-1}\ h^{-1}$ in subsequent experimental runs. Little loss in activity can be attributed to the loss of zinc from the catalyst which can be observed from the FTIR of the regenerated catalyst.

4 Conclusion

Zn–Al–M (M=Ca, Mg, La and Y) based ternary oxides were synthesized using two methods and their activity was studied for synthesis of DEC from EC. BET surface area of the catalysts prepared by the precipitation method was found to be more than that prepared by the impregnation method. This may be due to the plugging of pores of Zn–Al oxide by third element in the impregnation method. All the catalysts were found to posses strong basic sites. Yield of DEC was found to be in relation to the basicity of the catalysts. The ternary metal oxides prepared from the precipitation method were found to be more active

than the impregnation method. Zn–Al–Mg was found to be most active catalyst owing to its highly basic character. The activation of EC by catalyst was studied by carrying out FTIR spectra of EC interacted catalyst. Zn–Al–Mg catalyst prepared using liquid NH_3 as precipitant was also found to possess activity similar to Zn–Al–Mg precipitated from NaOH, although the latter was slightly more effective. Zn–Al–Mg prepared from precipitation method was found to be reusable three times with only 5% decline in its activity. Overall, DEC yield of 40.2% and turn over frequency (TOF) of 1055 $mg_{DEC}\ g_{cat}^{-1}\ h^{-1}$ was obtained in 5 h at 190 °C using ethanol/EC ratio of 10 with Zn–Al–Mg catalyst (10 wt% of EC). Overall, Zn–Al–Mg catalyst showed better yield and TOF than most of the studies reported on mixed oxides.

References

1. Behr A (1988) Angew Chem Int Edit 27:661–678
2. Zhang Y, Zhang S, Benson T (2015) Fuel Process Technol 131:7–13
3. Choi YJ, Sivanesan D, Lee J, Youn MH, Park KT, Kim HJ, Grace AN, Kim IH, Jeong SK (2016) J Ind Eng Chem 34:76–83
4. Kumar P, Srivastava VC, Gläser R, Mishra IM (2017) Powder Technol 309:13–21
5. Zhang Y, Zhang S, Lou HH, Gossage JL, Benson TJ (2014) Chem Eng Technol 37:1493–1499
6. Huang S, Liu S, Li J, Zhao N, Wei W, Sun Y (2006) Catal Lett 112:187–191
7. Tomishige K, Yasuda H, Yoshida Y, Nurunnabi M, Li B, Kunimori K (2004) Catal Lett 95:45–49
8. Eta V, Mäki-Arvela P, Salminen E, Salmi T, Murzin DY, Mikkola JP (2011) Catal Lett 141:1254
9. Kumar P, With P, Srivastava VC, Gläser R, Mishra IM (2017) J Alloy Compd 696:718–726
10. Schäffner B, Schäffner F, Verevkin SP, Börner A (2010) Chem Rev 110:4554–4581
11. Pacheco MA, Marshall CL (1997) Energy Fuel 11:2–29
12. Olmos RG, Iglesias M, Goenaga JM, Resa JM (2007) Int J Thermophys 28:1199–1227
13. Olmos RG, Iglesias M, Goenaga JM, Resa JM (2007) Phys Chem Liq 45:515–524
14. Shukla K, Srivastava VC (2017) Fuel Process Technol 161:116–124
15. Dunn BC, Guenneau C, Hilton SA, Pahnke J, Eyring EM, Dworzanski J, Meuzelaar HL, Hu JZ, Solum MS, Pugmire RJ (2002) Energy Fuel 16:177–181
16. Wang D, Yang B, Zhai X, Zhou L (2007) Fuel Process Technol 88:807–812
17. Zhang X, Jia D, Zhang J, Sun Y (2014) Catal Lett 144:2144–2150
18. Fan M, Zhang P, Ma X (2007) Fuel 86:902–905
19. Zhang P, Zhou Y, Fan M, Jiang P (2015) Appl Surf Sci 332:379–383
20. Zhang P, Zhou Y, Fan M, Jiang P (2014) Appl Surf Sci 295:50–53
21. Ma X, Fan M, Zhang P (2004) Catal Commun 5:765–770
22. Pimprom S, Sriboonkham K, Dittanet P, Föttinger K, Rupprechter G, Kongkachuichay P (2015) J Ind Eng Chem 31:156–166
23. Filippis PD, Scarsella M, Borgianni C, Pochetti F (2006) Energy Fuel 20:17–20
24. Fan M, Zhang P (2007) Energy Fuel 21:633–635
25. Kumar P, With P, Srivastava VC, Shukla K, Gläser R, Mishra IM (2016) RSC Adv 6:110235–110246
26. Keller T, Holtbruegge J, Górak A (2012) Chem Eng J 180:309–322
27. Shukla K, Srivastava VC (2016) RSC Adv 6:32624–32645
28. Shukla K, Srivastava VC (2017) Catal Rev 5:1–43
29. Lian G, Xinqiang Z, Hualiang A, Yanji W (2012) Chinese J Catal 33:595–600
30. Wang DF, Zhang XL (2012) Adv Mater Res 479:1768–1771
31. An H, Zhao X, Guo L, Jia C, Yuan B, Wang Y (2012) Appl Catal A 433:229–235
32. Qin XY, Liu B, Han B, Zhao WB, Wu SS, Lian PC (2013) Adv Mater Res 821:1081–1084
33. Wang L, Li H, Xin S, Li F (2014) Catal Commun 50:49–53
34. Xin S, Wang L, Li H, Huang K, Li F (2014) Fuel Process Technol 126:453–459
35. Wang P, Liu S, Zhou F, Yang B, Alshammari AS, Deng Y (2015) RSC Adv 5:19534–19540
36. Li F, Li H, Wang L, He P, Cao Y (2015) Catal Sci Technol 5:1021–1034
37. Wang D, Zhang X, Liu C, Cheng T, Wei W, Sun Y (2015) Appl Catal A 505:478–486
38. Zhao W, Feng D, Nong J, Cao G, Liu X, Tang Z, Chen Y (2016) React Kinet Mech Catal 117:639–654
39. Lee JH, Ko KH, Park BO (2003) J Cryst Growth (247:):119–125
40. Li J, Pan Y, Xiang C, Ge Q, Guo J (2006) Ceram Int 32:587–591
41. Siqingaowa Z, Yao H (2006) Front Chem China 1:277–280
42. ALOthman ZA (2012) Materials 5:2874–2902
43. Wei T, Wang M, Wei W, Sun Y, Zhong B (2003) Fuel Process Technol 83:175–182
44. Wang S, Zhao L, Wang W, Zhao Y, Zhang G, Ma X, Gong J (2013) Nanoscale 5:5582–5588
45. Rabiah-Nizah MF, Taufiq-Yap YH, Rashid U, Teo SH, Nur ZAS, Islam A (2014) Energy Convers Manag 88:1257–1262
46. Silambarasan M, Saravanan S, Soga T (2015) Phys E 71:109–116
47. Zappa D, Bertuna A, Comini E, Molinari M, Poli N, Sberveglieri G (2015) Anal Methods 7:2203–2209
48. Benson SW, Cruickshank FR, Golden DM, Haugen GR, O'neal HE, Rodgers AS, Shaw R, Walsh R (1969) Chem Rev 69:279–324
49. Zábranský M, Růžička VJ (2004) Phys Chem Ref Data 33:1071–1081